Lightest Higgs boson and relic neutralino in the MSSM with *CP* violation

Jae Sik Lee[1] and Stefano Scopel[2]

[1]*Center of Theoretical Physics, School of Physics, Seoul National University, Seoul, 151–747, Korea*
[2]*Korea Institute for Advanced Study, Seoul 130-722, Korea*

(Received 6 February 2007; published 2 April 2007)

We discuss the lower bound to the lightest Higgs boson H_1 in the minimal supersymmetric extension of the standard model with explicit *CP* violation, and the phenomenology of the lightest relic neutralino in the same scenario. In particular, adopting the CPX benchmark scenario, we find that the combination of experimental constraints coming from LEP, thallium electric dipole moment measurements, quarkonium decays, and $B_s \to \mu\mu$ decay favors a region of the parameter space where the mass of H_1 is in the range $7\ \text{GeV} \lesssim M_{H_1} \lesssim 10\ \text{GeV}$, while $3 \lesssim \tan\beta \lesssim 5$. Assuming a departure from the usual grand unified theory relation among gaugino masses ($|M_1| \ll |M_2|$), we find that through resonant annihilation to H_1 a neutralino as light as 2.9 GeV can be a viable dark matter candidate in this scenario. We call this the CPX light neutralino scenario and discuss its phenomenology showing that indirect dark matter searches are compatible with the present experimental constraints, as long as $m_\chi \lesssim M_{H_1}/2$. On the other hand, part of the range $m_\chi \gtrsim M_{H_1}/2$ which is allowed by cosmology is excluded by antiproton fluxes.

DOI: 10.1103/PhysRevD.75.075001 PACS numbers: 12.60.Jv, 14.80.Cp, 95.35.+d

I. INTRODUCTION

Supersymmetry (SUSY) is considered one of the most natural extensions of the standard model (SM), providing elegant solutions to puzzles as diverse as the SM hierarchy problem, the high-energy unification of the gauge coupling constants, and the existence of the dark matter (DM) in the Universe. In particular, in *R*-parity conserving SUSY scenarios the lightest neutralino turns out to be an ideal thermal DM candidate [1], providing in a natural way the correct amount of cold dark matter (CDM) that is needed to drive structure formation, and which is necessary to explain the latest data on the energy budget of the Universe from WMAP [2].

Unfortunately, our ignorance about the details of the SUSY-breaking mechanism implies that phenomenological analysis on the SUSY DM depend in general on a huge parameter space with more than 100 independent soft masses and couplings. This parameter space is usually drastically resized by making use of as many simplifying assumptions as possible. For instance, parameters related to flavor mixing are supposed to be strongly suppressed to match the experimental constraints, and are often neglected. On the other hand, in theoretically motivated setups as in specific SUSY-breaking scenarios, like in the minimal supergravity (SUGRA) [3], the number of free parameters is strongly reduced, improving predictability. However, some other assumptions are simply suggested by simplicity, such as taking soft-breaking parameters real.

In particular, many recent analyses have addressed this latter aspect [4–12], since it has been realized that *CP* violating phases in the soft terms can considerably enrich the phenomenology without violating existing constraints. This is also theoretically motivated by the fact that the smallness of neutrino masses implied by observation possibly calls for some exotic source of *CP* violation additional to Yukawa couplings, in order to explain baryogenesis.

In the *CP*-conserving SUGRA scenario, the so-called ''stau coannihilation,'' ''Higgs funnel,'' and ''focus point'' benchmark solutions are well-known examples of a situation where, thanks to a combination of different experimental constraints, quite simple and well-defined phenomenological pictures emerge, at the price of a certain amount of tuning [3]. In this article we point out that a similar situation occurs in an effective minimal supersymmetric extension of the standard model (MSSM) with all soft parameters fixed at the electroweak scale, when *CP* violation and departure from unification of gaugino masses are considered.

In particular, we wish to address here the issues of the lower bound for the mass of the lightest Higgs boson H_1 and that of the lightest possible mass for the relic neutralino χ, when standard assumptions are made for the origin and evolution of its relic density. In fact, by combining present experimental constraints, a very simple picture (albeit tuned) emerges, where the mass of the lightest Higgs boson H_1 is found to be in the range $7 \lesssim M_{H_1} \lesssim 7.5$ GeV, with the ratio of the two vacuum expectation values almost fixed, $\tan\beta \simeq 3$. This range can be relaxed to $7 \lesssim M_{H_1} \lesssim 10$ GeV and $3 \lesssim \tan\beta \lesssim 5$, with quite mild assumptions on the thallium electric dipole moment (EDM). In this scenario, resonant annihilations of neutralinos with mass $m_\chi \simeq M_{H_1}/2$ through H_1 exchange in the *s* channel can drive their thermal relic abundance within the limits coming from observation, for values of m_χ significantly below those allowed in *CP*-conserving scenarios [13] (to our knowledge, the issue of resonant χ annihilation in the context of *CP* violation was first raised at the qualitative level in [12]).

In the following we will analyze in detail the implications for direct and indirect DM searches of these light neutralinos, which we will refer to as the CPX light neutralino scenario, concluding that it is indeed a viable scenario, with prospects of detection in future experiments.

The plan of the paper is as follows. In Sec. II the CPX scenario in the MSSM with *CP* violation is introduced. In Sec. III we discuss various experimental bounds. Section IV is devoted to the discussion of the cosmological relic density of CPX light relic neutralinos, and Sec. V to their phenomenology in DM searches. Our conclusions are contained in Sec. VI.

II. MSSM WITH EXPLICIT *CP* VIOLATION: THE CPX SCENARIO

The tree-level Higgs potential of the MSSM is invariant under *CP* transformations. However, *CP* can be explicitly broken at the loop level. In the presence of sizable *CP* phases in the relevant soft SUSY-breaking terms, a significant mixing between the scalar and pseudoscalar neutral Higgs bosons can be generated [4–6]. As a consequence of this *CP*-violating mixing, the three neutral MSSM Higgs mass eigenstates, labeled in order of increasing mass as $M_{H_1} \leq M_{H_2} \leq M_{H_3}$, have no longer definite *CP* parities, but become mixtures of *CP*-even and *CP*-odd states. In this scenario, all masses are usually calculated as a function of the charged Higgs boson mass $M_{H^\pm}$, instead of the pseudoscalar Higgs mass M_A, which is no longer a physical parameter. Much work has been devoted to studying the phenomenological features of this radiative Higgs sector *CP* violation in the framework of the MSSM [7,8].

Because of the large Yukawa couplings, the *CP*-violating mixing among the neutral Higgs bosons is dominated by the contribution of third-generation squarks and is proportional to the combination

$$\frac{3}{16\pi^2}\frac{\Im\mathrm{m}(A_f\mu)}{m^2_{\tilde{f}_2}-m^2_{\tilde{f}_1}}, \tag{1}$$

with $f = t, b$. Here μ is the Higgs-mixing parameter in the superpotential and A_f denotes the trilinear soft coupling. In particular, the amount of *CP* violation is enhanced when the product of $|A_{b,t}|$ and $|\mu|$ is larger than the difference of the sfermion masses squared. At the two-loop level, also the gluino mass parameter M_3 becomes relevant through threshold corrections to the top- and bottom-quark Yukawa couplings. This contribution depends on the combination $\mathrm{Arg}(M_3\mu)$ and can be important especially when $\tan\beta \equiv v_2/v_1$ is large, where v_2 and v_1 are the vacuum expectation values of the neutral components of the two Higgs doublets that give masses to up-type and down-type quarks, respectively. More *CP* phases become relevant by including subdominant radiative corrections from other sectors [9].

In the presence of *CP* violation, the mixing among neutral Higgs bosons is described by a 3×3 real orthogonal matrix O, instead of a 2×2 one. The matrix O relates the electroweak states to the mass eigenstates as

$$(\phi_1, \phi_2, a)^T = O(H_1, H_2, H_3)^T. \tag{2}$$

We note that the elements $O_{\phi_1 i}$ and $O_{\phi_2 i}$ are the *CP*-even components of the ith Higgs boson, while O_{ai} is the corresponding *CP*-odd component.

The Higgs boson couplings to the SM and SUSY particles could be modified significantly due to the *CP* violating mixing. Among them, one of the most important ones may be the Higgs boson coupling to a pair of vector bosons, g_{H_iVV}, which is responsible for the production of Higgs bosons at e^+e^- colliders:

$$\mathcal{L}_{HVV} = gM_W\left(W^+_\mu W^{-\mu} + \frac{1}{2c^2_W}Z_\mu Z^\mu\right)\sum_{i=1}^{3} g_{H_iVV}H_i, \tag{3}$$

where

$$g_{H_iVV} = c_\beta O_{\phi_1 i} + s_\beta O_{\phi_2 i}, \tag{4}$$

when normalized to the SM value. Here we have used the following abbreviations: $s_\beta \equiv \sin\beta$, $c_\beta \equiv \cos\beta$. $t_\beta = \tan\beta$, etc. We note that the two vector bosons W and Z couple only to the *CP*-even components $O_{\phi_{1,2}i}$ of the ith Higgs mass eigenstate, and the relevant couplings may be strongly suppressed when the ith Higgs boson is mostly *CP* odd, $O^2_{ai} \sim 1 \gg O^2_{\phi_1 i}, O^2_{\phi_2 i}$.

The so-called CPX scenario has been defined as a showcase benchmark point for studying *CP*-violating Higgs-mixing phenomena [14]. Its parameters are all defined at the electroweak scale and are chosen in order to enhance the combination in Eq. (1). In this scenario, SUSY soft parameters are fixed as follows:

$$\begin{gathered} M_{\tilde{Q}_3} = M_{\tilde{U}_3} = M_{\tilde{D}_3} = M_{\tilde{L}_3} = M_{\tilde{E}_3} = M_{\mathrm{SUSY}}, \\ |\mu| = 4M_{\mathrm{SUSY}}, \qquad |A_{t,b,\tau}| = 2M_{\mathrm{SUSY}}, \\ |M_3| = 1\ \mathrm{TeV}, \end{gathered} \tag{5}$$

where, with a usual notation, Q, L, U, D, and E indicate chiral supermultiplets corresponding to left- and right-handed quarks and leptons. In this scenario $\tan\beta$, $M_{H^\pm}$, and M_{SUSY} are free parameters. As far as *CP* phases are concerned, we adopt, without loss of generality, the convention $\mathrm{Arg}(\mu) = 0$, while we assume a common phase for all the A_f terms, $\Phi_A \equiv \mathrm{Arg}(A_t) = \mathrm{Arg}(A_b) = \mathrm{Arg}(A_\tau)$. As a consequence of this, we end up with two free physical phases: Φ_A and $\Phi_3 = \mathrm{Arg}(M_3)$.

In addition to the parameters fixed by the CPX scenario, we need to fix the gaugino masses $M_{1,2}$ for our study. We take them as free parameters independently of M_3 since, for them, we chose to relax the usual relations at the electroweak scale: $M_i/M_j = g^2_i/g^2_j$ with $g_{i,j} =$ gauge coupling constants, which originate from the assumption of

gaugino-mass unification at the grand unified theory scale. The neutralino χ is defined as usual as the lowest-mass linear superposition of B-ino $\tilde{B}$, W-ino $\tilde{W}^{(3)}$, and of the two Higgsino states $\tilde{H}_1^0$, $\tilde{H}_2^0$:

$$\chi \equiv a_1\tilde{B} + a_2\tilde{W}^{(3)} + a_3\tilde{H}_1^0 + a_4\tilde{H}_2^0. \tag{6}$$

In Ref. [15] it was proved that in a CP-conserving effective MSSM with $|M_1| \ll |M_2|$ light neutralinos of a mass as low as 7 GeV are allowed. Indeed, for $|M_1| \ll |M_2|$ the LEP constraints do not apply, and the lower bound on the neutralino mass is set by the cosmological bound. As shown in [15], these neutralinos turn out to be mainly B-inos, $a_1 \simeq 1$ and $m_\chi \simeq |M_1|$, with a small Higgsino component given by

$$\frac{|a_3|}{|a_1|} \simeq \sin\theta_W \sin\beta \frac{M_Z}{|\mu|}, \tag{7}$$

where θ_W is the Weinberg angle and M_Z is the Z-boson mass. In the following we will assume vanishing phases for M_1 and M_2, and we will fix for definiteness $M_2 =$ 200 GeV (the phenomenology we are interested in is not sensitive to these parameters in a significant way). On the other hand, we will vary M_1, which is directly correlated to the lightest neutralino mass m_χ.

In this work, we rely on `CPsuperH` [16] for the computation of mass spectra and couplings in the MSSM Higgs sector.

III. EXPERIMENTAL CONSTRAINTS ON THE CPX SCENARIO

A. LEP2 searches

The most relevant feature of the CPX scenario for our analysis is that the lightest Higgs boson H_1 can be very light, $M_{H_1} \lesssim 10$ GeV, with the other two neutral Higgs bosons significantly heavier, $M_{H_{2,3}} \gtrsim 100$ GeV, when $\Phi_A \sim 90^o$ and $M_{H^\pm} \sim 130$ GeV for moderate values of $3 \lesssim \tan\beta \lesssim 10$. In this case, the lightest Higgs boson is mostly CP odd and its production at LEP is highly suppressed since $|g_{H_1VV}| \ll 1$ though it is kinematically accessible. On the other hand, the second-lightest Higgs H_2 can be produced together with a Z boson since its complementary coupling g_{H_2VV} is sizeable. But its mass is close to the kinematical limit $\sim$110 GeV and, moreover, it dominantly decays into two H_1's. Depending on M_{H_1}, the lightest Higgs boson decays into two b quarks or two τ leptons. This leads to a dominant production and decay mode containing 6 jets in the final state, a topology which was covered by LEP2 with a very low efficiency. The similar situation occurs for H_1–H_2 pair production. Therefore, in the presence of CP-violating mixings, a very light Higgs boson with $M_{H_1} \lesssim 10$ GeV could easily escape detection at LEP2.

For the CPX scenario, taking $\Phi_A = \Phi_3 = 90°$ and $M_{\rm SUSY} = 0.5$ TeV, the combined searches of the four LEP collaborations at $\sqrt{s} = 91$–209 GeV reported the following two allowed regions [17]:

$$\begin{aligned} &\textbf{R1}\text{: } M_{H_1} \lesssim 10 \text{ GeV} \quad \text{for } 3 \lesssim \tan\beta \lesssim 10, \\ &\textbf{R2}\text{: } 30 \text{ GeV} \lesssim M_{H_1} \lesssim 50 \text{ GeV} \quad \text{for } 3 \lesssim \tan\beta \lesssim 10. \end{aligned} \tag{8}$$

These regions will not be fully covered even at the LHC for $\tan\beta \lesssim 7$(**R1**) and $\lesssim 5$(**R2**) [18]. In our analysis we will focus on region **R1**.

We observe that in the scenario analyzed by the LEP collaborations one has $|\mu| = 2$ TeV. For this large value of $|\mu|$, the neutralino is a very pure B-ino configuration, with a Higgsino contamination $a_3 \simeq 0.02$ [see Eq. (7)]. As will be shown in Sec. IV, this has important consequences for the phenomenology of relic neutralinos, in particular, suppressing their annihilation cross section, and restricting the possibility of having a relic abundance in the allowed range only to the case of resonant annihilation. So, the exploration of different possibilities with lower values of $|\mu|$ could in principle be very relevant for relic neutralinos. However, this would require a reanalysis of LEP data which is beyond the scope of this paper.

B. Electric dipole moments

CP phases in the MSSM are significantly constrained by the EDM measurements. In particular, the EDM of the thallium atom provides currently the most stringent constraint on the MSSM scenario of our interest. The atomic EDM of ^{205}Tl gets its main contributions from two terms [19,20]:

$$\begin{aligned} d_{\rm Tl}[e\,{\rm cm}] = &-585 \cdot d_e[e\,{\rm cm}] - 8.5 \times 10^{-19}[e\,{\rm cm}] \\ &\cdot (C_S \text{ TeV}^2) + \cdots, \end{aligned} \tag{9}$$

where d_e denotes the electron EDM and C_S is the coefficient of the CP-odd electron-nucleon interaction $\mathcal{L}_{C_S} = C_S\bar{e}i\gamma_5 e\bar{N}N$. The dots denote subdominant contributions from six-dimensional tensors and higher-dimensional operators. The above quantity is constrained by the experimental 2-σ upper bound on the thallium EDM, which is [21]:

$$|d_{\rm Tl}| \lesssim 1.3 \times 10^{-24}[e\,{\rm cm}]. \tag{10}$$

The contributions of the first- and second-generation phases, e.g. $\Phi_{A_{e,\mu}}$, $\Phi_{A_{d,s}}$, etc., to EDMs can be drastically reduced either by assuming these phases sufficiently small, or if the first- and second-generation squarks and sleptons are sufficiently heavy. However, even when the contribution of the first- and second-generation phases to EDMs is suppressed, there are still sizeable contributions to EDMs from Higgs-mediated two-loop diagrams [22]. Their explicit forms for $(d_e/e)^H$ and C_S may be found in Ref. [23],

expressed in the conventions and notations of CPsuperH [16].

In Fig. 1, we show the rescaled thallium EDM $\hat{d}_{\rm Tl} \equiv d_{\rm Tl} \times 10^{24}$ in units of e cm in the M_{H_1}-$\tan\beta$ plane. Here, we consider only the contributions from the Higgs-mediated two-loop diagrams. Different ranges of $|\hat{d}_{\rm Tl}|$ are shown explicitly by different shadings. In the blank unshaded region we have obtained $|\hat{d}_{\rm Tl}| > 100$. We find that a cancellation between the contributions from $(d_e/e)^H$ and C_S occurs when $\tan\beta < 5$. This cancellation is responsible for the narrow region denoted by black squares with $|\hat{d}_{\rm Tl}| < 1$, where it is at the level of about 5%.

Finally, we note that the thallium EDM constraint can be evaded by assuming cancellations between the two-loop contributions considered here and other contributions, such as those from first- and second-generation sfermions discussed above. In this way the allowed region shown in Fig. 1 can be enlarged. The amount of cancellation can be directly read-off from Fig. 1. For instance, in the region $|\hat{d}_{\rm Tl}| < 10$ it would be less severe than 1 part in 10 (10%).

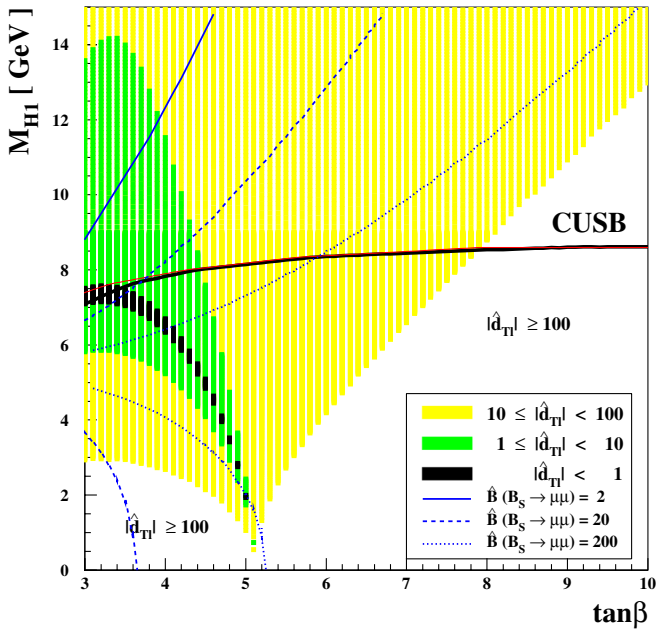

FIG. 1 (color online). The thallium EDM $\hat{d}_{\rm Tl} \equiv d_{\rm Tl} \times 10^{24}$ e cm in the CPX scenario with $M_{\rm SUSY} = 0.5$ TeV in the region $M_{H_1} \lesssim 15$ GeV and $3 < \tan\beta < 10$. The different shaded regions correspond to different ranges of $|\hat{d}_{\rm Tl}|$, as shown: specifically, the narrow region consistent with the current thallium EDM constraint, $|\hat{d}_{\rm Tl}| < 1$, is denoted by solid squares. In the blank unshaded region we have $|\hat{d}_{\rm Tl}| > 100$. The region below the thick solid line is excluded by data on $\Upsilon(1S)$ decay [25]. For comparison, the thin line shows an estimation of the same boundary obtained using the tree-level coupling taking $O_{a1} = 1$, i.e. $|g^P_{H_1\bar{b}b}| = \tan\beta$. Also shown are the three contour lines of the rescaled $\hat{B}(B_s \to \mu\mu) \equiv B(B_s \to \mu\mu) \times 10^7$: $\hat{B}(B_s \to \mu\mu) = 2$ (solid line), 20 (dotted line), and 200 (dashed line).

C. Bottomonium decay

In the region **R1**, see Eq. (8), the bottomonium decay channel $\Upsilon(1S) \to \gamma H_1$ is kinematically accessible [24]. There are two experimental limits on this process, depending on whether the H_1 decays to visible particles [25] or to invisible ones [26]. The second case is allowed when $2m_\chi < M_{H_1}$, so that H_1 can decay to neutralinos which escape detection. On the other hand, in the case $2m_\chi > M_{H_1}$ also the three-body decay (i.e. with a nonmonochromatic γ spectrum) $\Upsilon(1S) \to \gamma\chi\chi$ has been constrained [25]. The branching ratio for the two-body decay calculated in our scenario is related to its SM counterpart by [24]

$$B(\Upsilon(1S) \to \gamma H_1)_{\rm SUSY} = B(\Upsilon(1S) \to \gamma H_1)_{SM} \times (g^P_{H_1\bar{b}b})^2, \quad (11)$$

where $g^P_{H_1\bar{b}b}$ denotes the Higgs coupling to two b quarks given by $g^P_{H_1\bar{b}b} = -O_{a1}\tan\beta$ at the tree level. This implies that the experimental upper bounds on this process can be directly converted to a constraint in the plane $\tan\beta$-M_{H_1}. The result is shown in Fig. 1, where the thin (red) line corresponds to the limit obtained by setting $(g^P_{H_1\bar{b}b})^2 = \tan^2\beta$. Finite-threshold corrections induced by the gluino and chargino exchanges can modify the coupling $g^P_{H_1\bar{b}b}$, although this effect is negligible at low values of $\tan\beta$. Moreover, although for our choice of parameters H_1 is mostly pseudoscalar, O_{a1} can be smaller than 1 up to about 20%. The thick solid line in Fig. 1 shows the bottomonium constraint when the threshold corrections and O_{a1} are fully included.

From Fig. 1 one can see that, when the following constraints are combined, (i) the LEP constraint, (ii) thallium EDM, (iii) the limit from bottomonium decay, the allowed parameter space is reduced to

$$7\ \text{GeV} \lesssim M_{H_1} \lesssim 7.5\ \text{GeV} \quad \text{and} \quad \tan\beta \simeq 3. \quad (12)$$

This region may be enlarged to

$$7\ \text{GeV} \lesssim M_{H_1} \lesssim 10\ \text{GeV} \quad \text{and} \quad 3 \lesssim \tan\beta \lesssim 5, \quad (13)$$

if we assume 10%-level cancellation in the thallium EDM.

In light of the above discussion and for definiteness, from now on we will fix $M_{H_1} = 7.5$ GeV and $\tan\beta = 3$ in our analysis. Taking into account the CPX parameter choice of Eq. (5) with $\Phi_A = \Phi_3 = 90°$ and $M_{\rm SUSY} = 0.5$ TeV, this implies, in particular, $M_{H^\pm} \simeq 147$ GeV, $M_{H_2} \simeq 108$ GeV, $M_{H_3} \simeq 157$ GeV.

D. Other constraints

As will be discussed in the following sections, if the pseudoscalar Higgs boson mass is in the range (12), a CPX light neutralino with $m_\chi \lesssim M_{H_1}/2$ can be a viable DM candidate. Because of their very pure B-ino composition, and to the quite low value of $\tan\beta$, neutralinos in this mass

range evade constraints coming from accelerators. For instance, in the CPX light neutralino mass range the present upper bound to the invisible width of the Z boson implies $|a_3^2 - a_4^2| \lesssim$ a few percent, a constraint easily evaded in this case.

As far as flavor changing neutral currents (FCNC) are concerned, they strongly depend on the assumptions about flavor violation in the squark sector. For instance, assuming squarks diagonal in flavor, the SUSY contribution to the $b \to s\gamma$ decay rate is dominated by chargino-stop and $H^\pm - W$ loops, which are strongly suppressed in our case by the low value of $\tan\beta$ and by the fact that there are no light masses to compensate this.

The situation is potentially different in the case of the decay $B_s \to \mu\mu$, since its dominant SUSY contribution scales as $\tan^6\beta|\mu|^2/M_{H_1}^4$ and may have a resonance enhancement when H_1 is so light that $M_{H_1} \sim M_{B_s}$. Neglecting the threshold corrections which are not so important in our case, we estimate the branching ratio based on the approximated expression [27]

$$B(B_s \to \mu\mu) \simeq \frac{2\tau_{B_s} M_{B_s}^5 f_{B_s}^2}{64\pi}|C|^2(O_{\phi_1 1}^4 + O_{a1}^4) \qquad (14)$$

with

$$C \equiv \frac{G_F\alpha}{\sqrt{2}\pi} V_{tb}V_{ts}^* \left(\frac{\tan^3\beta}{4\sin^2\theta_W}\right)\left[\frac{m_\mu m_t|\mu|}{M_W^2(M_{H_1}^2 - M_{B_s}^2)}\right] \times \left(\frac{\sin 2\theta_{\tilde{t}}}{2}\right)\Delta f_3, \qquad (15)$$

where $\Delta f_3 = f_3(x_2) - f_3(x_1)$ with $x_i = m_{\tilde{t}_i}^2/|\mu|^2$ and $f_3(x) = x\log x/(1-x)$ and $\theta_{\tilde{t}}$ the stop mixing angle [28]. In Fig. 1, we show three contour lines of the rescaled $\hat{B}(B_s \to \mu\mu) \equiv B(B_s \to \mu\mu) \times 10^7$: $\hat{B}(B_s \to \mu\mu) = 2$ (solid line), 20 (dotted line), and 200 (dashed line). For the parameters chosen by combining the results from LEP2 searches, thallium EDM, and bottomonium decay, Eq. (12), we get $B(B_s \to \mu\mu)_{CPX} \simeq 6 \times 10^{-7}$ taking $f_{B_s} = 0.23$ GeV. This is 3 times larger than the present 95% C.L. limit [30]: $B(B_s \to \mu\mu) < 2 \times 10^{-7}$. This easily can be made consistent with the present experimental constraint if some mild cancellation takes place. The "GIM (Glashow-Iliopoulos-Maiani) operative point" mechanism discussed in Ref. [29] may be an example of such cancellation, when the squark mass matrices are flavor diagonal. In particular, we find that $B(B_s \to \mu\mu)_{CPX}$ is consistent to the experimental upper bound by choosing $0.8 \lesssim \rho \lesssim 0.9$, where $\rho \equiv m_{\tilde{q}}/M_{\rm SUSY}$ is the hierarchy factor introduced in Ref. [29], with $m_{\tilde{q}}$ the soft mass for squarks of the first two generations [31].

As far as the SUSY contribution to the anomalous magnetic dipole moment of the muon $\delta a_\mu^{\rm SUSY}$ is concerned, uncertainties in the SM make a comparison with the experimental results difficult. In particular, by combining the SM hadronic vacuum polarization results obtained from e^+e^- and $\tau^+\tau^-$ data, the SM calculation turns out to be compatible with observation, and the following 2-σ allowed interval for $\delta a_\mu^{\rm SUSY}$ is found [15]: $-160 \lesssim \delta a_\mu^{\rm SUSY} \times 10^{11} \lesssim 680$. The corresponding contribution from light neutralinos in the CPX scenario falls comfortably into this range: $\delta a_{\mu CPX}^{\rm SUSY} \times 10^{11} \simeq 1.5$ [to estimate this we have assumed for the trilinear coupling of the smuon the same value of the trilinear couplings of the third family given in Eq. (5)].

IV. THE RELIC DENSITY

Taking into account the latest data from the cosmic microwave data (CMB) combined with other observations [2] the 2-σ interval for the DM density of the Universe (normalized to the critical density) is

$$0.096 < \Omega_m h^2 < 0.122, \qquad (16)$$

where h is the Hubble parameter expressed in units of 100 km s^{-1} Mpc^{-1}. In Eq. (16) the upper bound on $\Omega_m h^2$ establishes a strict upper limit for the abundance of any relic particle. In particular, the neutralino relic abundance is given by the usual expression:

$$\Omega_\chi h^2 = \frac{x_f}{g_\star(x_f)^{1/2}} \frac{3.3 \cdot 10^{-38}\ \text{cm}^2}{\widetilde{\langle\sigma_{\rm ann} v\rangle}}, \qquad (17)$$

where $\widetilde{\langle\sigma_{\rm ann} v\rangle} \equiv x_f\langle\sigma_{\rm ann} v\rangle_{\rm int}$, $\langle\sigma_{\rm ann} v\rangle_{\rm int} \equiv \int_{T_0}^{T_f}\langle\sigma_{\rm ann} v\rangle dT/m_\chi$ being the integral from the present temperature T_0 up to the freeze-out temperature T_f of the thermally averaged product of the annihilation cross section times the relative velocity of a pair of neutralinos $\sigma_{\rm ann} v$, x_f is defined as $x_f \equiv \frac{m_\chi}{T_f}$, and $g_\star(x_f)$ denotes the relativistic degrees of freedom of the thermodynamic bath at x_f. For the determination of x_f we adopt a standard procedure [32].

In absence of some resonant effect, the natural scale of the annihilation cross section times velocity $\sigma_{\rm ann} v$ of CPX light neutralinos is far too small to keep the relic abundance below the upper bound of Eq. (16) (in particular they are very pure B-inos and their mass is below the threshold for annihilation to bottom quarks, which is usually the dominant channel of $\sigma_{\rm ann} v$ for light neutralinos [15]). However, when $m_\chi \simeq M_{H_1}/2$ neutralinos annihilate through the resonant channel $\chi\chi \to H_1 \to$ standard particles, bringing the relic abundance down to acceptable values. In the Boltzmann approximation the thermal average of the resonant $\sigma_{\rm ann} v$ to the final state f can be obtained in a straightforward way from the following relation among interaction rates:

$$\frac{n_\chi^2}{2}\langle\sigma_{\rm ann}v\rangle_{{\rm res},f} = \langle\Gamma(\chi\chi\to f)\rangle$$
$$= \langle\Gamma(\chi\chi\to H_1)B(H_1\to f)\rangle$$
$$= n_{H_1}\Gamma_\chi\frac{K_1(x_{H_1})}{K_2(x_{H_1})}B_f, \quad (18)$$

where brackets indicate thermal average, Γ_χ is the zero-temperature H_1 annihilation amplitude to neutralinos, and the thermal average of this quantity is accounted for by the ratio of modified Bessel functions of the first kind K_1 and K_2, B_f is the H_1 branching ratio to final state f, $n_i = g_i m_i^3 K_2(x_i)/(2\pi^2 x_i)$ are the equilibrium densities with $x_i = m_i/T$, T the temperature, and g_i the corresponding internal degrees of freedom, $g_\chi = 2$, $g_{H_1} = 1$. The factor of $1/2$ in front of Eq. (18) accounts for the identical initial states in the annihilation. From Eq. (18), and summing over final states f, one gets

$$\langle\sigma_{\rm ann}v\rangle_{\rm res} = \frac{\pi^2 M_{H_1}^2}{m_\chi^5}\frac{x_\chi K_1(x_{H_1})}{K_2^2(x_\chi)}\Gamma(H_1)B_\chi(1-B_\chi)$$
$$\times\Theta\left(\frac{x_{H_1}}{x_\chi}-2\right), \quad (19)$$

with $B_\chi = \Gamma_\chi/\Gamma(H_1)$, $\Gamma(H_1)$ the total decay amplitude of H_1, while Θ is the Heaviside step function [33].

By making use in Eq. (19) of the approximations $K_1(z) \simeq K_2(z) \simeq (\pi/(2z))^{1/2}\exp(-z)$, valid for $z \gg 1$, the integral over temperature can be done analytically, leading to

$$\langle\widetilde{\sigma_{\rm ann}v}\rangle_{\rm res} \simeq 4\pi^2\frac{x_f\Gamma(H_1)}{m_\chi^3}\frac{B_\chi(1-B_\chi)}{\beta_\chi}\sqrt{\frac{\delta(\delta+1)}{2}}$$
$$\times[1-erf(\sqrt{2(\delta-1)x_f})], \quad (20)$$

where $\delta \equiv M_{H_1}/(2m_\chi)$, $\beta_\chi = \sqrt{1-\delta^{-2}}$, and $erf(x) = 2/\sqrt{\pi}\int_0^x \exp(-t^2)dt$.

The result of our calculation is shown in Fig. 2, where the neutralino relic abundance $\Omega_\chi h^2$ is shown as a function of the mass m_χ. In this calculation the annihilation cross section has been calculated including the off-resonance contribution to the annihilation cross section. In this way we have checked that, for $m_\chi < M_{H_1}/2$, $\langle\widetilde{\sigma_{\rm ann}v}\rangle_{\rm res}$ is always the dominant contribution in the calculation of $\Omega_\chi h^2$, and Eq. (20) is an excellent approximation of $\langle\widetilde{\sigma_{\rm ann}v}\rangle$. The off-resonance contribution to the annihilation cross section is also responsible for regularizing the relic density for $m_\chi > M_{H_1}/2$, where $\langle\widetilde{\sigma_{\rm ann}v}\rangle_{\rm res}$ is vanishing. The asymmetric shape of the curve in Fig. 2 is due to the fact that thermal motion allows neutralinos with $m_\chi < M_{H_1}/2$ to reach the center-of-mass energy needed to create the resonance, while this is not possible for $m_\chi > M_{H_1}/2$. In the same figure, the two horizontal lines indicate the range of

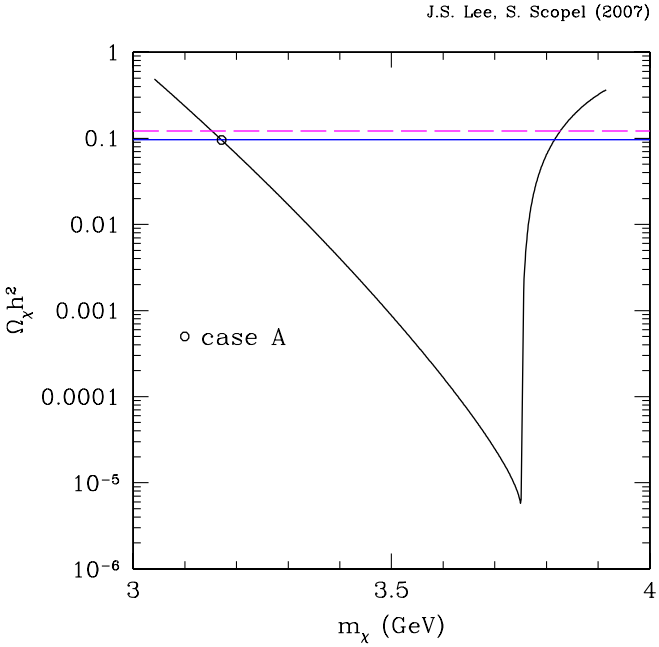

FIG. 2 (color online). Relic abundance as a function of the neutralino mass m_χ for the CPX scenario with $M_{H_1} = 7.5$ GeV, $\tan\beta = 3$, $M_{\rm SUSY} = 0.5$ TeV, and $\Phi_A = \Phi_3 = 90°$. The two horizontal lines indicate the interval of Eq. (16). The circle, where $\Omega_\chi h^2 = (\Omega_m h^2)_{\rm min}$, is discussed as "case A" in Sec. V.

Eq. (16). The point shown as a circle and indicated as "case A" will be used in the following section as a representative point to calculate some signals.

In Fig. 2 the neutralino mass range allowed by cosmology is $3.15\ {\rm GeV} \simeq m_\chi \simeq 3.83\ {\rm GeV}$. Allowing for the variation of M_{H_1} within the range of Eqs. (12) and (13), this range is enlarged to

$$2.93\ {\rm GeV} \lesssim m_\chi \lesssim 5\ {\rm GeV}. \quad (21)$$

In this scenario the neutralino relic abundance can fall in the range of Eq. (16) only with some level of tuning at the boundaries of the allowed mass range. For intermediate values of m_χ either the neutralino is a subdominant component of the DM, or some nonthermal mechanism for its cosmological density needs to be introduced. Of course all our considerations are valid if standard assumptions are made about the evolution of the early Universe (e.g. about the reheating temperature at the end of inflation, the energy budget driving Hubble expansion, entropy production, etc.).

V. DARK MATTER SEARCHES

Neutralinos are CDM particles, and are supposed to clusterize at the galactic level. This implies that they can provide the DM density which is gravitationally measured in our Galaxy. In particular, in this section we will assume for the DM density in the neighborhood of the solar system the reference value $\rho_0 = 0.3\ {\rm GeV/cm^3}$. When we com-

pare our calculation of $\Omega_\chi h^2$ to the interval of Eq. (16), we interpret the lower bound on the DM relic density $(\Omega_m h^2)_{\rm min} = 0.096$ as the average abundance below which the halo density of a specific CDM constituent has to be rescaled as compared to the total CDM halo density. So, whenever $\Omega_\chi h^2 < (\Omega_m h^2)_{\rm min}$ we assume that neutralinos provide a local density ρ_χ which is only a fraction of ρ_0. For the determination of the rescaling factor $\xi \equiv \rho_\chi/\rho_0$ we adopt the standard recipe:

$$\xi = \min[1, \Omega_\chi h^2/(\Omega_m h^2)_{\rm min}]. \tag{22}$$

Neutralinos in the halo of our Galaxy can be searched for through direct and indirect methods. In particular, CPX light neutralinos are quite hard to detect through direct detection. Direct detection consists in the measurement of the elastic scattering of neutralinos off the nuclei of a low-background detector. For the mass range of Eq. (21), the most stringent upper bound on the neutralino-nucleon coherent elastic cross section $\sigma_{\rm scalar}^{\rm (nucleon)}$ is provided by the CRESST-1 experiment [35], $\sigma_{\rm scalar}^{\rm (nucleon)} \lesssim 10^{-38}$ cm^2 [36]. This value is much above the cross section expected in our scenario, which falls in the range $(\sigma_{\rm scalar}^{\rm (nucleon)})_{CPX} \simeq 10^{-42}$ cm^2. This is due to the fact that the neutralino-Higgs coupling which dominates this process is suppressed, since $\tan\beta$ is small and χ's are very pure B-inos due to the large value of $|\mu|$. Moreover, $\sigma_{\rm scalar}^{\rm (nucleon)}$ is dominated by the exchange of scalar Higgs bosons, while H_1 is mostly pseudoscalar. Finally, contrary to annihilation, no resonant enhancement is present in the elastic cross section, since scattering proceeds through the t channel.

For this reason, in this section we concentrate on the indirect detection of CPX light neutralinos. In our scenario the neutralino relic density $\Omega_\chi h^2$ is driven below the observational limit by the resonant enhancement of the annihilation cross section $\langle\widetilde{\sigma_{\rm ann} v}\rangle$. The same cross section calculated at present times, $\langle\sigma_{\rm ann} v\rangle_0$, enters into the calculation of the annihilation rate of neutralinos in our galaxy. This could produce observable signals, like γ's, ν's or exotic components in cosmic rays, like antiprotons, positrons, antideuterons.

Note, however, that one can have $\langle\sigma_{\rm ann} v\rangle_0 \ll \langle\widetilde{\sigma_{\rm ann} v}\rangle$. In fact, as already shown in Sec. IV, the thermal motion in the early Universe ($x_\chi \simeq x_f \simeq 20$) allows neutralino resonant annihilation when $m_\chi < M_{H_1}/2$. However, for the same neutralinos the contribution of the resonance to $\langle\sigma_{\rm ann} v\rangle_0$ can be negligible at present times, since their temperature in the halo of our Galaxy is of order $x_{\chi,0} \simeq 10^{-6} \ll x_f$. This implies that the annihilation cross section can be large enough in the early universe in order to provide the correct relic abundance, but not so large at present times as to drive indirect signals beyond observational limits.

In the following we will discuss expected signals for γ rays and antiprotons. The results of our analysis are summarized in Figs. 3–6. In all figures observables are calculated in the CPX scenario with $M_{H_1} = 7.5$ GeV, $\tan\beta = 3$, $M_{\rm SUSY} = 0.5$ TeV, and $\Phi_A = \Phi_3 = 90°$, and plotted as a function of the neutralino mass m_χ. The solid lines show our results obtained by adopting the rescaling procedure for the local density explained above, while for comparison, dashed lines are calculated assuming $\rho_\chi = \rho_0$. When rescaling is applied, indirect signals are proportional to the combination $\xi\rho_\chi^2\langle\sigma_{\rm ann} v\rangle_0$, so they reach their maximum value when $\Omega_\chi h^2 = (\Omega_m h^2)_{\rm min}$.

For all our results we have adopted, as a reference model, a Navarro-Frenk-White (NFW) profile for the DM density:

$$\rho(r) = \rho_0 \frac{(r_0/a)^\gamma[1 + (r_0/a)^\alpha]^{(\beta-\gamma)/\alpha}}{(r/a)^\gamma[1 + (r/a)^\alpha]^{(\beta-\gamma)/\alpha}}, \tag{23}$$

where $r_0 = 8.5$ kpc is the distance of the solar system from the galactic center (GC), $a = 25$ kpc is the core radius, while $(\alpha, \beta, \gamma) = (1, 3, 1)$.

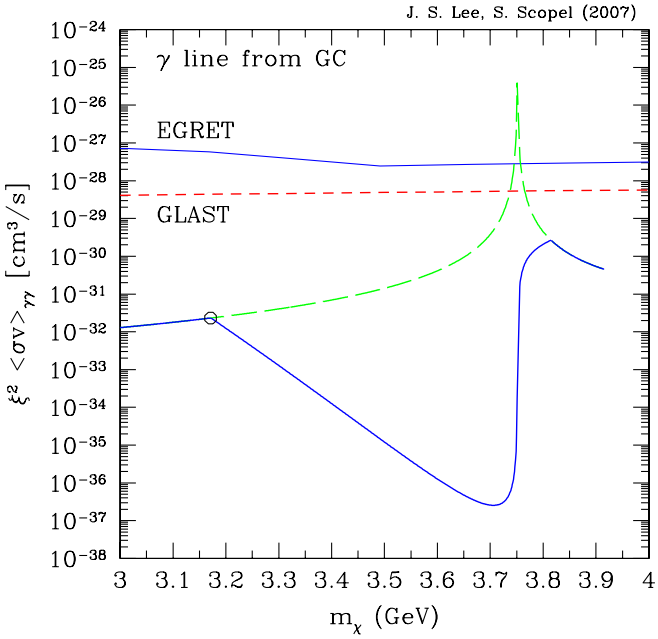

FIG. 3 (color online). Rescaled, zero-temperature neutralino-annihilation cross section to two photons, as a function of m_χ. For the solid line the rescaling factor ξ is calculated according to Eq. (22), while for the dashed one $\xi = 1$. The solid horizontal line shows the corresponding constraint from a search for a γ line from the GC from EGRET [41]. The dashed horizontal line is an estimate for the sensitivity of GLAST [52] for a similar search, when model $A - N2$ of Ref. [43] is used to extrapolate HESS data to lower energies. Circle: see caption of Fig. 2.

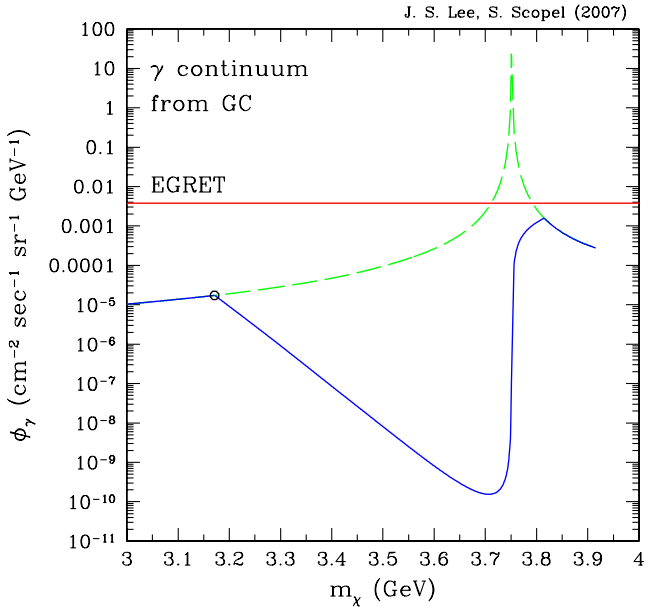

FIG. 4 (color online). Continuum γ flux from the GC calculated for $E_\gamma = 122$ MeV. For the solid line the neutralino local density is rescaled according to Eq. (22), while for the dashed one, $\xi = 1$. The fluxes are compared to the corresponding measurement from EGRET [45], shown as the horizontal solid line. Circle: see caption of Fig. 2.

A. Gamma flux from the galactic center

In Figs. 3 and 4 we show our results for a γ signal from the GC, which is the most promising source of γ's from neutralino annihilation. Note that signals from the GC are proportional to the line-of-sight integral (i.e., performed on a path pointing from the observer to the γ source) $\bar{J} \equiv 1/\Delta\Omega \int_{l.o.s.} \rho_\chi^2 dl d\Omega$, where Ω is the pointing angle of observation in the sky and $\Delta\Omega$ is the experimental angular resolution. The quantity $\bar{J}$ is very sensitive to the particular choice of density profile and may span several orders of magnitude, especially for those models that diverge in the origin, as for the NFW, where a cutoff radius $r_{\rm cut}$ is needed [40]. In particular, in our calculation we use $r_{\rm cut} = 10^{-2}$ pc.

The γ signal from neutralinos takes two contributions: a line with $E_\gamma = m_\chi$, produced by direct annihilation of χ's to two γ's, and a continuum, which is mainly due to the annihilation of π^0's produced in the fragmentation and decay of other final states (quarks, gluons, and τ's).

In the first case, the zero-temperature annihilation cross section of neutralinos to photons $\langle \sigma_{\rm ann} v \rangle_{0,\gamma\gamma}$ is usually suppressed, since it takes place at the one-loop level. However, in our case the contribution of the H_1 resonance, $\chi\chi \to H_1 \to \gamma\gamma$ can lead to a strong enhancement of the

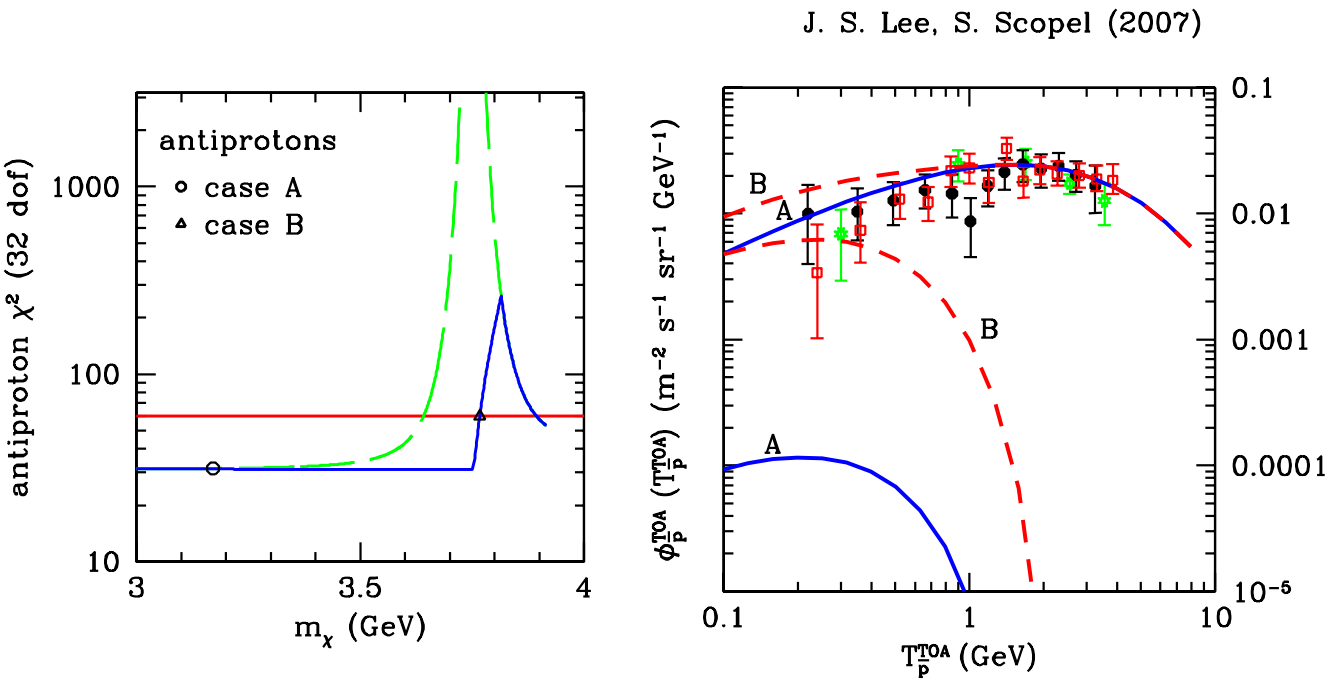

FIG. 5 (color online). Left: χ^2 calculated for the top-of-atmosphere $\bar{p}$ flux compared to the experimental data from the BESS and AMS collaborations [49] (explicitly shown in the right-hand panel). For the solid line the neutralino local density is rescaled as explained in Sec. V. For the dashed one, $\xi = 1$. The solid horizontal line indicates the 99.5% C.L. upper bound for the χ^2. The comparison of the χ^2 with its upper limit allows one to set an upper bound to m_χ, indicated by case B and shown as a triangle. On the other hand the circle indicates case A, introduced in Fig. 2. Right: top-of-atmosphere antiproton flux as a function of the kinetic top-of-atmosphere energy of $\bar{p}$'s, for the cases A (solid curve) and B (dashed curve), shown in the left panel as a circle and a triangle, respectively. In both cases the lower curve shows the contribution from primaries produced by neutralino annihilation, while the upper curve is the total flux where the primary contribution is added to the standard secondary one. The 32 experimental points [49] are the same that are used to calculate the χ^2 shown in the left-hand panel: full circles: BESS 1995-97; open squares: BESS 1998; stars: AMS.

signal, as is evident from Fig. 3, where our calculation of $\xi^2\langle\sigma_{\rm ann}v\rangle_{0,\gamma\gamma}$ is compared to the upper bound (horizontal solid line) on the same quantity from EGRET [41] (such analysis has been performed on a region of $10^\circ \times 10^\circ$ around the GC, which, for our assumptions, implies $\bar{J} \simeq 120$ GeV^2 cm^{-6} kpc). In this figure the solid line shows our result when ξ^2 is calculated according to Eq. (22), while for the dashed line $\xi = 1$.

In the same figure we also show with a horizontal dashed line an estimate for the prospect of detection of the same quantity with GLAST (the Gamma Ray Large Area Telescope) (in this case we have assumed an angular resolution of $\Delta = 10^{-5}$ sr in the calculation of $\bar{J}$, leading to $\bar{J} \simeq 2500$). This estimate is somewhat uncertain, since HESS [42] has detected a TeV source of γ's in the GC which is likely to be of standard origin, representing a background for DM searches, and potentially making detection of new physics in that region more difficult [43]. Our estimate of the background is obtained by extrapolating the HESS source to lower energies by using the model $A - N2$ described in [43] (we have made the same assumptions also to estimate the horizontal solid line in Fig. 6). Our choice of model $A - N2$ is optimistic, since it implies the smallest extrapolated background at low energies among those discussed in [43]. Of course, a more conservative choice for the model adopted to explain the HESS source could make prospects of DM detection for GLAST in the GC much worse.

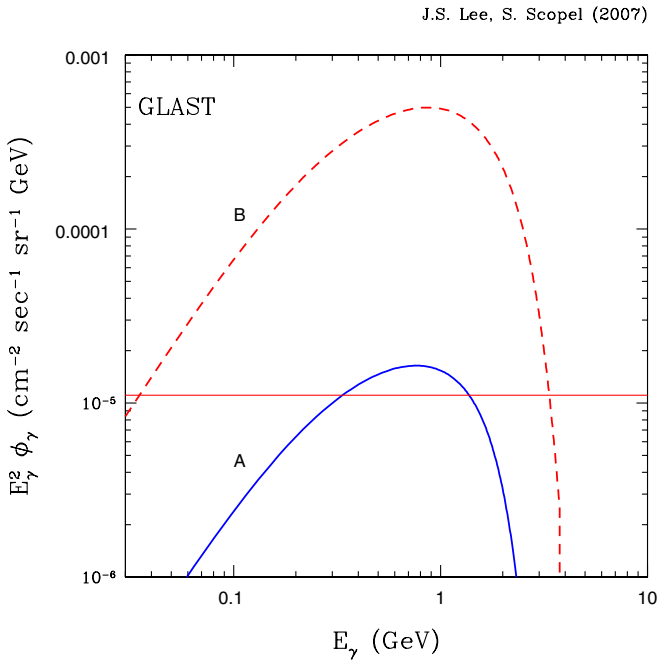

FIG. 6 (color online). Expected signal for GLAST [52] for a gamma continuum flux from the galactic center as a function of the γ energy for the cases A (solid curve) and B (dashed curve) indicated in Figs. 2–4 as a circle and a triangle, respectively. The horizontal line is an estimate of the background for GLAST (see text).

As far as the continuum signal is concerned, we have calculated the γ yield from the final states of neutralino annihilation using PYTHIA [44]. The result of the calculation is shown in Fig. 4, where we have evaluated the γ flux ϕ_γ from the GC for $E_\gamma = 122$ MeV and compared it with the corresponding flux measurement from EGRET [45], shown as a horizontal solid line (this particular energy bin is within the range where the data are well fitted by a standard background. In this case the flux has been measured in an angular region of $10^\circ \times 4^\circ$ around the GC, which corresponds, for our choice of parameters, to $\bar{J} \simeq 184$ GeV^2 cm^{-6} kpc).

From Figs. 3 and 4 we can conclude that, with reasonable choices for the DM density profile, γ signals in our scenario are compatible with observations. In both figures we have indicated with a circle the point indicated as "case A" in Fig. 2.

B. Antiproton flux

As far as light neutralinos are concerned, a particularly stringent limit is provided by the flux of primary antiprotons that are produced from the hadronization of neutralino-annihilation final states [46–48]. This is due to the fact that the $\bar{p}$ flux observed experimentally is quite in agreement with that expected from $\bar{p}$ secondary production from cosmic rays [49], so that not much room is left for exotic contributions. Moreover, as all other annihilation processes, the primary neutralino signal scales with the neutralino number density $\propto 1/m_\chi^2$, so it is enhanced for light masses. However, once they are produced in the DM halo, primary $\bar{p}$'s interact with the magnetic field of the Galaxy, and a complex propagation model is needed in order to calculate the fraction of them that reaches the Earth. Unfortunately, the main parameters of the propagation model are fixed by using secondary cosmic rays data (such as the B/C ratio) which mainly depend on the galactic disk, while primary $\bar{p}$'s from neutralino annihilation are produced in the galactic halo. This induces uncertainties in the primary flux as large as 2 orders of magnitude [47]. In particular, for our analysis we have used the public code provided by Ref. [48] for the $\bar{p}$ propagation. Although the code of Ref. [48] is a simplified one, where, in particular, energy-redistribution effects are neglected, it serves well our needs for checking the viability of our scenario. In the left panel of Fig. 5 we show the χ^2 calculated by comparing the sum of the primary and secondary top-of-atmosphere $\bar{p}$ fluxes to the experimental data from the BESS and AMS collaborations. In particular, for the calculation of the χ^2 we have used the same 32 data points from BESS 1995-97, BESS 1998, and AMS 1998 [49] shown in the right panel. For our calculation we have used a solar modulation parameter $\phi = 500$ MV, corresponding to the period of minimal solar activity when these

experiments have taken data. Moreover, in order to be conservative, we have used the minimal propagation model in Table III of Ref. [48], i.e. $\delta = 0.85$, $K_0 = 0.0016\ \mathrm{kpc}^2\,\mathrm{Myr}^{-1}$, $L = 1$ kpc, $V_c = 13.5\ \mathrm{km}/s$, and $V_A = 22.4\ \mathrm{km}/s$ for the propagation parameters δ and K_0, for the size of the diffusion zone L, and for the galactic wind V_c. In absence of a SUSY contribution we find $\chi^2 \simeq 30$, which confirms the good agreement between the data and the standard secondary production (for this latter flux we use the quantity calculated in [48]). As a conservative upper bound for the χ^2 we take $\chi^2 = 60$, which for 32 degrees of freedom implies a statistical disagreement at the level of 99.5%. This value is shown in Fig. 5 as a solid horizontal line.

From Fig. 5 one can see that, even when the rescaled neutralino local density is used, the χ^2 from $\bar{p}$ data exceeds 60 for $m_\chi \simeq 3.77$ GeV. This values for the neutralino mass is indicated with a triangle (case B), along with the circle which indicates case A introduced in Fig. 2. Both cases are shown in the right-hand panel, where the upper curves show the total $\bar{p}$ fluxes, while the lower curves show the SUSY contributions.

From the discussion of this section, where $m_{H_1} = 7.5$ GeV and $\tan\beta = 3$, we obtain for m_χ the allowed range: $3.15\ \mathrm{GeV} \lesssim m_\chi \lesssim 3.77$ GeV. The boundaries of this range correspond to the cases A and B introduced previously. Assuming for M_{H_1} and $\tan\beta$ the range of Eqs. (12) and (13) this interval for m_χ is enlarged to $2.93\ \mathrm{GeV} \lesssim m_\chi \lesssim 5$ GeV.

We conclude this section by showing and example for the prospects of detection for cases A and B in future DM searches: in Fig. 6 the γ continuum flux from the GC is estimated for GLAST (we have assumed here an angular resolution of $\Delta = 10^{-5}$ sr in the calculation of $\bar{J}$, leading to $\bar{J} \simeq 2500$). This flux is compared to an estimate of the background for the same detector, shown as a horizontal line, calculated with the same assumptions as in Fig. 3, where model $A - N2$ of Ref. [43] is used to extrapolate HESS data to lower energies.

VI. CONCLUSIONS

In the present paper we have discussed the lower bound to the lightest Higgs boson H_1 in the MSSM with explicit CP violation and the phenomenology of the lightest relic neutralino in the same scenario. In particular, we have examined the parameter space region $M_{H_1} \lesssim 10$ GeV and $3 \lesssim \tan\beta \lesssim 10$, in the CPX scenario, an interval which has not been excluded by the combined searches of the four LEP collaborations. We find that the combination of experimental constraints coming from thallium EDM measurements and quorkonium decays restricts the region allowed by LEP to $7\ \mathrm{GeV} \lesssim M_{H_1} \lesssim 7.5$ GeV, $\tan\beta \simeq 3$. In this range, the branching ratio $B(B_s \rightarrow \mu\mu)$ is compatible to the present experimental upper bounds provided some moderate cancellation is allowed between the stop-loop contribution and that of other squarks. Furthermore, the allowed parameter space can be relaxed to $7\ \mathrm{GeV} \lesssim M_{H_1} \lesssim 10$ GeV and $3 \lesssim \tan\beta \lesssim 5$ if a cancellation less severe than 1 part in 10 is also assumed in thallium EDM between two-loop contributions and, for example, those depending on first- and second-generation phases.

For the above choice of parameters and assuming a departure from the usual grand unified theory relation among gaugino masses ($|M_1| \ll |M_2|$) we find that neutralinos with $2.9\ \mathrm{GeV} \lesssim m_\chi \lesssim 5$ GeV can be viable DM candidates. We refer to them as CPX light neutralinos. In particular, in the CPX scenario the neutralino is a very pure B-ino configuration, suppressing its Higgs-mediated cross sections. However, through resonant annihilation to H_1 the thermal relic density of neutralinos with $m_\chi \simeq M_{H_1}/2$ can be either tuned within the range compatible to WMAP or virtually erased, allowing for alternative nonthermal mechanisms. The cosmologically allowed range for m_χ extends to $m_\chi \lesssim M_{H_1}/2$ due to the effect of the thermal motion in the early universe. We also have discussed the phenomenology of CPX light neutralinos, showing that signals for indirect dark matter searches are compatible with the present experimental constraints, as long as $m_\chi \lesssim M_{H_1}/2$. On the other hand, part of the range $m_\chi \gtrsim M_{H_1}/2$ allowed by cosmology is excluded by antiproton fluxes.

Finally, we note that our study shares some generic features with other models such as the next-to-minimal supersymmetric model, in which a light Higgs boson may escape LEP searches and the observed amount of DM is explained through neutralino resonant annihilation [50,51].

ACKNOWLEDGMENTS

The work of J. S. L. was supported in part by the Korea Research Foundation (KRF) and the Korean Federation of Science and Technology Societies Grant and in part by the KRF Grant No. KRF-2005-084-C00001 funded by the Korea Government (MOEHRD, Basic Research Promotion Fund). S. S. would like to thank A. Bottino for useful discussions.

[1] For some recent reviews, see, for instance D. J. H. Chung, L. L. Everett, G. L. Kane, S. F. King, J. D. Lykken, and L. T. Wang, Phys. Rep. **407**, 1 (2005); G. Jungman, M. Kamionkowski, and K. Griest, Phys. Rep. **267**, 195 (1996), and references therein.

[2] D. N. Spergel *et al.*, astro-ph/0603449.

[3] V. Berezinsky, A. Bottino, J. R. Ellis, N. Fornengo, G. Mignola, and S. Scopel, Astropart. Phys. **5**, 1 (1996); J. R. Ellis, K. A. Olive, Y. Santoso, and V. C. Spanos, Phys. Lett. B **565**, 176 (2003); M. Battaglia, A. De Roeck, J. R. Ellis, F. Gianotti, K. A. Olive, and L. Pape, Eur. Phys. J. C **33**, 273 (2004); R. Arnowitt, B. Dutta, and B. Hu, hep-ph/0310103.

[4] A. Pilaftsis, Phys. Rev. D **58**, 096010 (1998); Phys. Lett. B **435**, 88 (1998).

[5] A. Pilaftsis and C. E. M. Wagner, Nucl. Phys. **B553**, 3 (1999); D. A. Demir, Phys. Rev. D **60**, 055006 (1999); S. Y. Choi, M. Drees, and J. S. Lee, Phys. Lett. B **481**, 57 (2000); M. Carena, J. Ellis, A. Pilaftsis, and C. E. M. Wagner, Nucl. Phys. **B586**, 92 (2000); **B625**, 345 (2002).

[6] S. Heinemeyer, Eur. Phys. J. C **22**, 521 (2001); M. Frank, T. Hahn, S. Heinemeyer, W. Hollik, H. Rzehak, and G. Weiglein, hep-ph/0611326.

[7] E. Accomando *et al.*, hep-ph/0608079.

[8] J. R. Ellis, J. S. Lee, and A. Pilaftsis, Mod. Phys. Lett. A **21**, 1405 (2006).

[9] T. Ibrahim and P. Nath, Phys. Rev. D **63**, 035009 (2001); **66**, 015005 (2002); S. W. Ham, S. K. Oh, E. J. Yoo, C. M. Kim, and D. Son, Phys. Rev. D **68**, 055003 (2003).

[10] T. Nihei, Phys. Rev. D **73**, 035005 (2006).

[11] G. Belanger, F. Boudjema, S. Kraml, A. Pukhov, and A. Semenov, Phys. Rev. D **73**, 115007 (2006).

[12] P. Gondolo and K. Freese, J. High Energy Phys. 07 (2002) 052.

[13] A. Bottino, F. Donato, N. Fornengo, and S. Scopel, Phys. Rev. D **68**, 043506 (2003).

[14] M. Carena, J. R. Ellis, A. Pilaftsis, and C. E. M. Wagner, Phys. Lett. B **495**, 155 (2000).

[15] A. Bottino, N. Fornengo, and S. Scopel, Phys. Rev. D **67**, 063519 (2003).

[16] J. S. Lee, A. Pilaftsis, M. Carena, S. Y. Choi, M. Drees, J. R. Ellis, and C. E. M. Wagner, Comput. Phys. Commun. **156**, 283 (2004).

[17] G. Abbiendi *et al.* (OPAL Collaboration), Eur. Phys. J. C **37**, 49 (2004); OPAL Physics Note PN505, http://opal.web.cern.ch/Opal/pubs/physnote/html/pn505.html; A. Heister *et al.* (ALEPH Collaboration), Phys. Lett. B **526**, 191 (2002); J. Abdallah *et al.* (DELPHI Collaboration), Eur. Phys. J. C **32**, 145 (2004); P. Achard *et al.* (L3 Collaboration), Phys. Lett. B **545**, 30 (2002); P. Bechtle, in Ref. [7].

[18] M. Schumacher, in Ref. [7].

[19] I. B. Khriplovich and S. K. Lamoreaux, *CP Violation Without Strangeness* (Springer, New York, 1997).

[20] For a recent review, see, M. Pospelov and A. Ritz, Ann. Phys. (N.Y.) **318**, 119 (2005).

[21] B. C. Regan, E. D. Commins, C. J. Schmidt, and D. DeMille, Phys. Rev. Lett. **88**, 071805 (2002).

[22] For two-loop Higgs-mediated contributions to EDMs in the *CP*-violating MSSM, see D. Chang, W.-Y. Keung, and A. Pilaftsis, Phys. Rev. Lett. **82**, 900 (1999); A. Pilaftsis, Nucl. Phys. **B644**, 263 (2002); D. A. Demir, O. Lebedev, K. A. Olive, M. Pospelov, and A. Ritz, Nucl. Phys. **B680**, 339 (2004); K. A. Olive, M. Pospelov, A. Ritz, and Y. Santoso, Phys. Rev. D **72**, 075001 (2005).

[23] J. R. Ellis, J. S. Lee, and A. Pilaftsis, Phys. Rev. D **72**, 095006 (2005).

[24] J. F. Gunion, H. E. Haber, G. Kane, and S. Dawson, *The Higgs Hunter's Guide* (Perseus Publishing, Cambridge, MA, 1990).

[25] P. Franzini *et al.*, Phys. Rev. D **35**, 2883 (1987).

[26] R. Balest *et al.* (CLEO Collaboration), Phys. Rev. D **51**, 2053 (1995).

[27] T. Ibrahim and P. Nath, Phys. Rev. D **67**, 016005 (2003).

[28] Following the calculation in Ref. [29], one might get a different expression than that of Eq. (14), in that the branching ratio would scale as $(O^2_{\phi_1 1} + O^2_{a1})^2$.

[29] A. Dedes and A. Pilaftsis, Phys. Rev. D **67**, 015012 (2003).

[30] A. Abulencia *et al.* (CDF Collaboration), Phys. Rev. Lett. **95**, 221805 (2005); **95**, 249905(E) (2005); D. Acosta *et al.* (CDF Collaboration), Phys. Rev. Lett. **93**, 032001 (2004); V. M. Abazov *et al.* (D0 Collaboration), *ibid.* **94**, 071802 (2005); A. Abulencia *et al.* (CDF Collaboration), Phys. Rev. Lett. **95**, 221805 (2005); **95**, 249905(E) (2005).

[31] To be consistent with the present $B(B_s \to \mu\mu)$ limit, one may take a point in the region above the $\hat{B}(B_s \to \mu\mu) = 2$ line in Fig. 1 where one needs a cancellation in the thallium EDM. We note that an appropriate choice of the phases $\Phi_{A_{e,\mu}}$, $\Phi_{A_{d,s}}$ always allows to make the parameter region of Eq. (13) consistent with the thallium EDM constraint when $\rho \simeq 0.9$. We keep Eq. (12) as our reference point, assuming cancellation in $B(B_s \to \mu\mu)$.

[32] E. W. Kolb and M. S. Turner, *The Early Universe* (Addison Wesley, Reading, MA, 1990).

[33] Our result for $\langle \sigma_{\rm ann} v \rangle_{\rm res}$ is a factor of 2 larger than the corresponding expression calculated in [34]. We explain this discrepancy with the fact that in [34] the Breit-Wigner expression of the cross section, Eq. (6.1), should be a factor 2 larger, to compensate for a factor $1/2$ contained in the decay amplitude of the resonance to 2 (identical) neutralinos.

[34] P. Gondolo and G. Gelmini, Nucl. Phys. **B360**, 145 (1991).

[35] J. Jochum *et al.*, Nucl. Phys. B, Proc. Suppl. **124**, 189 (2003); G. Angloher *et al.*, Yad. Fiz. **66**, 521 (2003) [Phys. At. Nucl. **66**, 494 (2003)].

[36] We remind that the DAMA Collaboration measures an annual modulation effect [37], compatible to what was expected by relic neutralinos in some supersymmetric models [38] or by other dark matter candidates [39]. The model discussed in the present paper provides elastic cross sections too low to explain the DAMA modulation effect.

[37] R. Bernabei *et al.*, Riv. Nuovo Cimento **26N1**, 1 (2003).

[38] A. Bottino, F. Donato, N. Fornengo, and S. Scopel, Phys. Rev. D **69**, 037302 (2004).

[39] R. Bernabei *et al.*, Int. J. Mod. Phys. A **21**, 1445 (2006).

[40] N. Fornengo, L. Pieri, and S. Scopel, Phys. Rev. D **70**, 103529 (2004).

[41] A. R. Pullen, R. R. Chary, and M. Kamionkowski, astro-ph/0610295.

[42] F. Aharonian *et al.* (HESS Collaboration), Astron. Astrophys. **425**, L13 (2004).

[43] G. Zaharijas and D. Hooper, Phys. Rev. D **73**, 103501 (2006).
[44] T. Sjostrand, S. Mrenna, and P. Skands, J. High Energy Phys. 05 (2006) 026.
[45] S. D. Hunger *et al.*, Astrophys. J. **481**, 205 (1997).
[46] A. Bottino, F. Donato, N. Fornengo, and S. Scopel, Phys. Rev. D **70**, 015005 (2004).
[47] A. Bottino, F. Donato, N. Fornengo, and P. Salati, Phys. Rev. D **58**, 123503 (1998); **72**, 083518 (2005).
[48] D. Maurin, R. Taillet, and C. Combet, astro-ph/0609522. To calculate the $\bar{p}$ propagation we have used the code provided by the authors at the link http://wwwlapp.in2p3.fr/~taillet/mtc/mtc_code.tar.
[49] S. Orito *et al.* (BESS Collaboration), Phys. Rev. Lett. **84**, 1078 (2000); T. Maeno *et al.* (BESS Collaboration), Astropart. Phys. **16**, 121 (2001); M. Aguilar *et al.* (AMS Collaboration), Phys. Rep. **366**, 331 (2002); **380**, 97 (2003).
[50] F. Ferrer, L. M. Krauss, and S. Profumo, Phys. Rev. D **74**, 115007 (2006).
[51] J. F. Gunion, D. Hooper, and B. McElrath, Phys. Rev. D **73**, 015011 (2006); R. Dermisek, J. F. Gunion, and B. McElrath, hep-ph/0612031.
[52] See for instance, www-glast.slac.stanford.edu/software/IS/glast_lat_performance.htm.